# Resonant Instabilities in Synchrotron Accelerators from Space Charge Effects

M. B. Ottinger
Truman State University
Kirksville, MO 63501

T. Tajima
University of Texas
Austin, TX 78703

K. Hiramoto
Power & Industrial Systems R&D Division.
Hitachi-shi, Ibaraki-ken, 316, Japan

Running Title: Synchrotron Resonant Instabilities

Address: Michael B. Ottinger
161 Barnett Hall
Truman State University
100 E. Normal
Kirksville, MO 63501

fax: (660)-785-76040
e-mail: ottinger@truman.edu

# ABSTRACT

The space-charge effects of low-energy Gaussian beams in synchrotron accelerators can significantly affect the beam particle trajectories, including altering the regions of beam instability. We show that the tuneshift of a Gaussian beam is not uniform throughout the beam, but decreases as a function of particle amplitude. From the amplitude dependence of the tuneshift, we derive equations for the region of beam instability due to integer resonances and coupled resonances. We demonstrate the validity of these equations through particle simulation.



Keywords: Instability, Synchrotron, Space-charge, Integer Resonance, Coupled Resonance

## INTRODUCTION

A major concern of beam dynamics in synchrotron accelerators at low energies (such as in low energy injectors/boosters and medical proton accelerators) is the deleterious effects of space charge[1, 2,3]. Unlike in the relativistic energy regime, at lower energies the repulsive electrostatic force of protons is not compensated by the self-induced magnetic force. For intense beams, this repulsive force leads to substantial changes in the beam dynamics, including a shift in the tune (the number of transverse oscillations made by the beam particles as they make a complete revolution around the synchrotron). Since the external magnetic force (from the synchrotron magnets) gives rise to the stable betatron oscillation characterized by the tune, the electrostatic force that counteracts this magnetic force yields to a reduction of the tune, this is, a negative tuneshift. Many beam instabilities are associated with beam tune resonances, so it is important to understand how the space charge affects the tune, and in turn these resonances. To study this phenomenon, we examine the evolution of the kinetic radial beam distribution using our newly developed self-consistent space charge particle-in-cell code.

## TUNESHIFT IN BEAM WITH GAUSSIAN PROFILE

It has long been known that beams with rational tunes are unstable due to nonlinear effects, even without the addition of space charge[4]. Without space charge, the tune (also called the design tune) is fixed by the lay out of the synchrotron magnets. The addition

of space charge modifies the tunes of the individual particles and, therefore, changes the region of instability (range of design tunes for which the beam is unstable).

The most common method for calculating the tuneshift is by assuming a constant, uniform density beam. The space charge force then becomes a linear function of radius, yielding a radially independent tuneshift, known as the Laslett tuneshift[5]

$$\Delta\nu_o = -\frac{ISe}{8\pi\gamma^2 m\beta^2 c^3 \varepsilon_n}, \tag{1}$$

where I is the beam current, S is the length of the ideal particle trajectory around the synchrotron, e is the particle charge, $\gamma$ and $\beta$ are the relativistic factors, m is the mass of the particle, c is the speed of light, and $\varepsilon_n$ is the normalized beam emittance (area occupied by the beam in phase space). According to the Laslett tuneshift, all particles within the beam have the same shifted tune. The tune has its greatest negative shift when the beam is at low energies (small $\gamma$ and $\beta$) and approaches the unshifted tune as the beam is accelerated to high energies. Theoretically, if during the acceleration process, the tune passes through a rational value, the beam becomes unstable.

In most synchrotron machines, the beams violate the premises of Laslett tuneshift, in that they are not uniform density, but have Gaussian radial profiles. Some modifications to the Laslett tuneshift have been proposed to account for discrepancies between the Laslett tuneshift and the average tuneshifts from real beams[6]. These corrections still only discuss the average tuneshift, and not the spreading of the individual particle tunes. As a result, the evaluation of the tune-shift remains art, rather than science.

For a non-uniform density beam, such as a Gaussian beam, the tuneshift is a function of the amplitude of the transverse oscillations. For an azimuthally symmetric Gaussian beam with radial density profile, the tuneshift can be written as[7]

$$\Delta\nu = \frac{eIS}{4\pi\gamma^2\beta^2c^3\varepsilon_n}\left(\frac{1-e^{-A}}{A}\right), \tag{2}$$

where A is the particle amplitude given by

$$A = \frac{\gamma\beta}{2\varepsilon_n}\left\langle\frac{x^2}{\beta_{cs}}\right\rangle, \tag{3}$$

with $\left\langle\frac{x^2}{\beta_{cs}}\right\rangle$ being the variance of the particle trajectory from the ideal orbit.

Equation (2) has a finite maximum value at A=0,

$$\Delta\nu_{\max} = \frac{eIS}{4\pi\gamma^2\beta^2c^3\varepsilon_n}, \tag{4}$$

and drops off to zero as the amplitude increases. The maximum tuneshift is twice the Laslett tuneshift, as would be expected, since the central density of a Gaussian beam is twice the density of a uniform beam under similar conditions. The average tuneshift is calculated by averaging the amplitude dependent tuneshift weighted by the density profile ($e^{-A}$), over all possible amplitudes,

$$\Delta\nu_{avg} = \ln(2)\Delta\nu_{\max} \approx 1.38\Delta\nu_o. \tag{5}$$

Although Eq. (5) gives a specific value for the average tuneshift, it is not the average tuneshift which causes resonant instabilities, but the tunes of each individual

particle. Since, as Eq. (2) shows, the tuneshift ranges from the maximum tuneshift to zero, we expect any beam whose tuneshift crosses a resonant value to increase in amplitude. In the subsequent sections, we demonstrate through computer simulation that, while the tuneshift is spread over a large range, the scarcity of particles at large amplitudes and a redistribution of particles due to resonance, enables a beam to partially cross a rational tune without becoming totally unstable.

## SIMULATION ALGORITHM

We developed a self-consistent computer model[8] to track a set of macro-particles around the synchrotron lattice in full 6-dimensional phase space. For a long, lattice dominated beam with slowly varying radial profile the space-charge force has only a radial component and can be calculated using a two-dimensional algorithm. The synchrotron magnets are applied as thin-elements as described by Schachinger and Talman[9], and used in similar codes, such as SIMPSONS[10]. This method reduces the synchrotron accelerator to a series of drift regions separated by thin magnets. The methods of particle and momentum advancement for the drift regions and magnetic elements are explained separately.

### Advancement through Drift Regions

In the drift region the electric and magnetic fields are from the particle space-charge (no external fields). To advance the particles we use a modified Euler method. Each particle is advanced in space a timestep dt, according to the equations

$$
\begin{aligned}
x^{n+1} &= x^n + \beta_x^n c\, dt \\
y^{n+1} &= y^n + \beta_y^n c\, dt \\
s^{n+1} &= s^n + \beta_s^n c\, dt,
\end{aligned}
\tag{6}
$$

where x, y, and s are the horizontal, vertical, and longitudinal positions. The space-charge electric field at each particle is calculated using a standard two-dimensional particle-in-cell algorithm with a Fourier transform, to solve Poisson's equation, and linear interpolation between grids, similar to a model developed by Chen[11]. Using the resulting fields, the particle momenta are advanced as

$$
\begin{aligned}
\beta_x^{n+1} &= \beta_x^n + \frac{E_x}{\gamma^3} dt \\
\beta_y^{n+1} &= \beta_y^n + \frac{E_y}{\gamma^3} dt \\
\beta_s^{n+1} &= \beta_s^n + \frac{\beta_s^n}{\gamma^3} (\beta_x^n E_x + \beta_y^n E_y) dt.
\end{aligned}
\tag{7}
$$

## Regions with Synchrotron Magnets

When there is a thin element in a particle's path during the time step, the particle is advanced in time, $dt_1$, to the element and there the particle momentum receives its magnetic kick as

$$
\begin{aligned}
\beta_x^+ &= \beta_x^- - \frac{\beta_s}{1+\delta} \xi_y \\
\beta_y^+ &= \beta_y^- + \frac{\beta_x}{1+\delta} \xi_x \\
\beta_s^+ &= \sqrt{(\beta_s^-)^2 + (\beta_x^-)^2 + (\beta_y^-)^2 - (\beta_x^+)^2 - (\beta_y^+)^2}.
\end{aligned}
\tag{8}
$$

The parameter $\delta$ is the particle's fractional deviation from the design momentum and $\xi$ is calculated from the particle's position and the magnetic poles ($a_n$, $b_n$) as

$$
\xi_x + i\xi_y = \sum_{n=0}^{n_{poles}} (b_n + a_n)(x + iy)^n. \tag{9}
$$

Using the new momentum the particle is then advanced in space for the remainder of the timestep ($dt_2$=dt-$dt_1$).

### Data Acquisition

Using this algorithm, a set of macro-particles, usually 4096, is advanced around the synchrotron lattice for a given number of turns. As each particle completes a full cycle in the synchrotron, its transverse position and momentum are used to calculate the particle's amplitude and tune, as well as the beam's rms emittance and average tune. From these parameters we observe how varying initial conditions affect the beam emittance and radial distribution.

## REGIONS OF INSTABILITY

Resonant instabilities occur when integral multiples of the transverse tunes sum to an integral value,

$$m\nu_x + n\nu_y = k, \tag{10}$$

where m,n, and k are integers[4]. When both m and n are non-zero, the resonance is called a coupled resonance, and when either m or n is zero, it is a rational resonance. We examine the regions of instability for both of these resonances separately in the next sections.

### Region of Rational Resonance Instability

We first consider the non-coupled, or rational resonance. Here, the particles' transverse oscillations are synchronous with the longitudinal synchrotron period. The

synchronicity allows magnetic errors (unplanned glitches in the magnetic elements) to affect the particle trajectories without decay through phase mixing. This leads to instability in the particle orbits and to increases in the beam emittance.

When there is no space charge, the beam tune is independent of the particle amplitude. A resonant particle increases in amplitude until it reaches an aperture and is lost. Without space charge, all particles have the same tune, and therefore this instability may be avoided by selecting an irrational value for the design tune.

When space charge is significant, Eq. (2) shows that the beam tune is spread over a finite region ranging from the machine tune (at A=∞), to the maximum tuneshift below the machine tune (at A=0). To avoid the resonant instability a design tune should be selected such that no particles are resonant. The region of instability associated with the resonance n/m then lies in the range

$$n/m < \nu_d < n/m + \Delta\nu_{\max} \tag{11}$$

where $\nu_d$ is the design tune.

There are two factors, however, that can significantly decrease the size of this region. First, the inequality on the left-hand-side of Eq. (11) is a result of large amplitude particles. According to Eq. (2), as the amplitude increases the tuneshift goes to zero. However, for a Gaussian beam, the density of particles at large amplitudes also goes to zero. When the amplitude is sufficiently large, the particle density becomes low enough that any lost particles are insignificant. Secondly, the inequality on the right-hand-side of Eq. (11) accounts for particles at small amplitudes. When these particles increase in

amplitude, they can restabilize as they move away from the unstable amplitudes. This produces a change in the beam's radial profile, but no particles are lost. Using our computer simulation, we examined the limits on the region of instability and modified Eq. (11) to account for these two factors.

Before we examine the limits on the region of instability, we look at the parameters that affect the region of instability. Equation (4) shows three primary parameters which affect the maximum tuneshift: the beam current (I), the beam energy ($\gamma^2\beta^2$), and the beam emittance ($\varepsilon_n$). To verify that the region of instability is a function of the tuneshift, and not these parameters individually, we perform three sets of simulation runs. In each set of runs, the design tunes are varied from 1.01 to 1.15 to observe the region associated with the integer resonance (n/m=1). Each simulation run lasts 500 turns and the relative final emittance (final emittance divided by initial emittance) are plotted as a function of design tune. The maximum tuneshift is kept constant over the three runs, while the current, energy, and emittance are varied. The resulting amplitude growths as a function of design tune are shown in Fig. 1. Within uncertainty, all three regions of uncertainty coincide. For the remainder of our simulations we keep the emittance and energy constant, and vary the current.

Next, we see that the region of instability is affected by the magnitude of the space charge tuneshift. A series of runs using four different currents is completed for a range of design tunes with the final relative emittances plotted for each current. Figure 2 shows that the size and location (away from the rational design tune) of the region of instability are proportional to the current, and therefore the tuneshift. It is important to

note that for the smallest design tunes within the instability the emittance has the greatest growth, while the growth tapers off slowly as the design tune is increased. Also, the beam is stable for regions slightly above the resonance, whereas, Eq. (11) predicted all regions above the resonance would be unstable. Finally, the instability does not extend completely out to a value of the maximum tuneshift above the resonance, but gradually diminishes before it.

## Adjusting the lower limit of the region of instability

Since the tuneshift theoretically decreases to zero at large particle amplitudes [See Eq. (2)], when a beam with design tune above the integer has a maximum tuneshift extending part of the beam tune below the integer, some particles are always found in the unstable region. However, we see that for sufficiently large tuneshifts, beams with design tunes slightly above the integer are stable. In these cases the particles with integral tunes are at amplitudes many times larger than the *rms* amplitude. Since the beam has a Gaussian distribution, there are few particles in this region. When these particles become unstable and are lost, they do not significantly affect the beam. In practice only beams with significant number of particles overlapping the resonance will become unstable.

We can modify Eq. (11) to exclude this region since there are too few particles to affect the beam emittance. Although the outer limit of this region does not have a definite value, we chose eight times the *rms* amplitude as a sufficient cut-off point, or :

$$\Delta\nu_{\max}\frac{1-e^{-8}}{8}\approx 0.125\Delta\nu_{\max}. \tag{12}$$

This region of instability then becomes:

$$n/m+0.125\Delta\nu_{\max}<\nu_d<n/m+\Delta\nu_{\max}. \tag{13}$$

## Adjusting the upper limit of the region of instability

Without space charge, the resonance is independent of beam size and resonant particles increase in amplitude until they hit the synchrotron wall and are lost. When space charge is included in the instability, the emittance grows by a finite value, due to the instability, before becoming stable again.

For the series of simulation runs, shown in Fig. 2 with current of 0.5 Amperes, we plot the emittance growth as a function of turn, Fig. 3(a), and the average vertical beam tune as a function of turn, Fig. 3(b). From the emittance growth we see that for the unstable cases, the amplitude increases by a finite amount before restabilizing. Comparing the amplitude growth to the average tune, we see that the restabilization corresponds to the time when the average tune achieves a value slightly above the resonance. The largest emittance growth (for the case of $\nu_{yo}$=1.05) corresponds to the largest change in tuneshift required for the beam tune to move above the integer.

This limit on the instability is explained by the redistribution of particles within the beam. Since the space charge tuneshift depends on the particle amplitude, the resonant particles only increase in amplitude by a finite amount before their tunes

become stable. Since the tuneshift also depends on the beam size, or emittance, as the unstable particles increase in amplitude they also change the beam emittance. This larger emittance decreases the total tuneshift, making particles at smaller amplitudes resonant. Over time the instability increases the amplitudes of all beam particles, as necessary, until all are above the resonance. At this time the beam is again stable.

Depending upon what amplitude particles are resonant, the rational resonance is be divided into two groups, or classifications: beam growth and beam redistribution. To distinguish between these two classes, we show, in Fig. (4), scatterplots of the initial (first turn) and final (500th turn) particle tune as a function of particle amplitude for machine tunes $\nu_{yo}$=1.01, 1.05, 1.09, and 1.15. Along side these are the initial and final radial beam profiles for each tune. In each case we use a beam with a current of 0.50 amps, energy of 10 MeV, emittance of $10\pi$ mm-mrad, and horizontal machine tune of 1.75.

In the first case, $\nu_{yo}$=1.01, the tuneshift decreases the initial total tune of each particle below the integer resonance. Since all of the particles have tunes below the resonance, no particles are unstable, so no beam growth occurs. In this case the initial and final tune distributions are similar [Fig. 4(a) and (b)] and radial profile [Fig. 4(c)] also remains unchanged.

For the second case, $\nu_y$=1.05, the large amplitude particles initially have tunes which lay across the integer resonance [Fig. 4(d)]. Since the tuneshift changes only slightly at large amplitudes, the resonant particles are able to increase significantly in amplitude before either becoming lost to the system, or restabilizing at a significantly

larger amplitude. This redistribution of particles decreases the tuneshifts of smaller amplitude particles, causing them to also become resonant. The final result is an increase in the total beam size, and the loss of many particles [Fig. 4(e)]. The final radial profile, Fig. 4(f), shows that the beam size increases significantly while the density becomes more uniform over the entire beam.

The third case, $\nu_y$=1.09, the initial tune distribution, Fig. 4(g) shows that the large amplitude particles are above the integer tune, while the smaller amplitude particles cross the resonance. From Fig. 4(h) we see little change in the tune distribution of large amplitude particles, but a shift of small amplitude particles into the larger amplitude region. The final radial profile, Fig. 4(i), shows a shift in particles to larger amplitudes creating a more uniform distribution.

In the fourth case, $\nu_y$=1.15, all the particles initially have tunes above the integer resonance [Fig. 4(j)]. Since no particles are resonant, no growth occurs and the final tune distribution and radial profiles remains the same [Fig. 4(k) and (l)].

From this survey we see that beam growth occurs only when some of the particles have resonant tunes. When the total tunes of all particles lie below the integer resonance, Figs. 4(a)-(c), or the total tunes of all particles lie above the integer resonance, Figs. 4(j)-(l), no beam growth occurs. When the large amplitude particles lie across the resonance, Figs. 4(d)-(f), the beam size increases and particles are lost. Here the greatest beam emittance growth occurs, as all particles increase in size until the beam is sufficiently spread out that the total tune of each particle is above resonance. Finally, when the small

amplitude particles are resonant but the large amplitude particles are stable, Figs. 4(g)-(i), the total beam size does not increase, but the beam distribution changes until all particles are above the resonance.

Since the resonance of small amplitude particles (A<1) does not cause a significant loss of particles, nor an increase in the maximum beam size, we exclude these resonances from our region of instability. The maximum tuneshift for resonant particles becomes

$$\Delta\nu_{\max}\frac{1-e^{-1}}{1}\approx 0.632\Delta\nu_{ma}. \tag{14}$$

This makes the effective region of instability:

$$n/m+0.125\Delta\nu_{\max}<\nu_d<n/m+0.632\Delta\nu_{\max}. \tag{15}$$

Studying the integer resonance, we find that the region of instability is a function of the space charge tuneshift, associated with the amplitude spread in tune and is given by Eq. (15). The instability is due to the individual particle resonance, as the beam restabilizes when particle tunes move above the resonance. Finally, we see that the resonance could be divided into two types: beam growth with particle loss, and beam redistribution. The region of beam redistribution is excluded from the region of instability as it does not cause a change in maximum beam size.

## Coupled Resonance

The second major resonant instability is the coupled resonance which occurs when integral multiples of the transverse tunes sum to an integer,

$$a\nu_x + b\nu_y = c \tag{16}$$

where a, b, and c are integers[4]. Not all combinations of coupled resonances are unstable. In fact, only cases where a+b≤4 have been shown to be unstable. To observe the effects of the space charge in the resonance we will look at the unstable case with a=1, b=2, and c=4.

Since this resonance is a function of both the horizontal and vertical tunes, and both are affected by the space charge, this resonance is more complex than the rational resonance of the previous section when space charge is included. To understand the nature of this instability, we first look at the width of the region without space charge. Then we show how the space charge modifies the region and produce an equation showing the two-dimensional region of instability.

### Coupled resonance without space charge

Our main concern in examining this instability without space charge is to find the width of the instability, and the dependence of that width on the particle amplitude. This was accomplished using the particle routine TEAPOT[9], which tracks individual particles of known amplitude through the synchrotron lattice. By running the simulation for lattices with horizontal machine tunes of 1.75, while varying the vertical machine tune

around 1.125 and varying the particle amplitude, we are able to determine three regions associated with the coupled resonance. Figure 5, shows these regions. The first region is closest to the resonant tune and grows in width with increasing amplitude. Particles that start within this region have amplitudes which grow exponentially [See tunes 1.125, 1.126, and 1.127 of Fig. 6]. The rate of growth increases the closer the tune is to the resonant value. The second region surrounds the first. Particles that begin in this region have oscillating amplitudes [See tunes 1.128, 1.129, 1.130, 1.135, and 1.150 of Fig. 6]. The oscillation frequency and amplitude decrease as the particle begins further away from the resonance.

The behavior of the amplitude in the region of resonance leads to the empirical equation

$$A(N_\tau) = A_o + \Delta A \frac{Sin\left(N_\tau \sqrt{|\nu_r - \nu| - \Delta\nu_c}\right)}{\sqrt{|\nu_r - \nu| - \Delta\nu_c}} \tag{17}$$

where $\nu$ is the vertical tune, $\nu_r$ is the resonant tune, $\Delta\nu_c$ is the distance between the resonant tune and the boundary between exponential growth and oscillatory motion, $A_o$ is the average amplitude, $\Delta A$ is the oscillation amplitude at $\nu=\nu_c$, and $N_\tau$ is the turn number. In the region where the tune is between the resonant tune and the critical tune, the argument of the Sine function is imaginary (switching it to a Hyperbolic Sine). This provides to the expected exponential growth. In the region of oscillation as the tune moves further away from the critical tune the frequency of oscillation increases while the magnitude diminishes.

This study shows that the coupled resonance without space charge has a finite range over which it affects the particle amplitude. This range can be broken down into a region of exponential growth and one of oscillatory motion and that the width of these regions increases with particle amplitude.

## Coupled resonance with space charge

As we have shown previously, space charge in a Gaussian beam decreases the tune of each particle, with the amount of tuneshift dependent upon the particle amplitude. Particles with the smallest amplitudes have the largest tuneshifts. To observe how the space charge affects the coupled resonance we use a series of runs with a current of 0.20 amps and energy 10 MeV. The horizontal emittance is set at $50\pi$ mm-mrad, while the vertical emittance is $10\pi$ mm-mrad. The larger horizontal emittance minimizes the spread in horizontal tune. The horizontal machine tune is set to 1.75 and with an average space charge tuneshift of 0.012. Three vertical machine tunes are used (1.12, 1.14, and 1.16) with an average tuneshift of 0.033.

Figure 7 shows the results of the simulation using a vertical machine tune of 1.12. As the top two graphs show, the initial tune/amplitude distribution does not significantly change during the 200 turn simulation. The lower graph shows the individual particle amplitudes as a function of turn. A few particles developed oscillatory amplitudes and two particles were been lost. However, most of the particles maintained a constant amplitude. This is considered to be a stable region.

Figure 8 shows the same three views for a simulation with a machine tune of 1.14. In this case, many of the large amplitude particles initially fall into the unstable and oscillatory regions which gives rise to many lost particles. As in the integer resonance case, when the large amplitude particles are lost, the tune of the smaller amplitude particles increases, making them also become resonant. As Fig. 8 shows after a period of 200 turns many particles are lost, and those remaining fall into the oscillatory or exponential regions. Due to the large particle loss this is the most unstable region.

Figure 9 shows the beam evolution with an initial machine tune of 1.15. The initial distribution shows many particles in the unstable region. However, since the tune of large amplitude particles lie above the resonance, in either a stable or an oscillatory region, as the beam evolves the unstable particles move into the oscillatory and stable regions. Figure 9 shows that no particles are lost in this case, but due to the oscillatory motion of many particles the average beam emittance has increased.

## Region of coupled instability

Before a region of instability can be defined, we must first define what it means to be unstable. Does it mean any growth in emittance? Or does it mean lost particles? Since the regions bounding the exponential growth and the oscillatory growth have the same shape, either definition of stability can be accounted for, by using one of two definitions for the width of the range of unstable tunes ($\delta\nu$). When only the exponential growth region is desired, $\delta\nu$ should be the width of the exponential region ($\delta\nu_{exp}$). When

the oscillatory region is to be included, $\delta\nu$ should be the width of the oscillatory region ($\delta\nu_{osc}$).

Applying the finite width of the region of instability ($\delta\nu$) to Eq. (16), we get the range of tunes for which the beam will be resonant,

$$a(\nu_x - \delta\nu_x) + b(\nu_y - \delta\nu_y) < c < a(\nu_x + \delta\nu_x) + b(\nu_y + \delta\nu_y), \tag{18}$$

where $\delta\nu_x$ and $\delta\nu_y$ are the widths of the region of instability ($\delta\nu_{exp}$ or $\delta\nu_{osc}$).

Each particle tune can be rewritten as the design tune minus the amplitude dependant tuneshift

$$\nu = \nu_o - \Delta\nu_{\max} \frac{(1 - e^{-A})}{A}. \tag{19}$$

To find the maximum and minimum effective tunes we can impose the same limits that we did for the rational resonances. Resonant particles with amplitudes smaller than the *rms* amplitude (A=1) experience some growth, but after redistribution of amplitudes, they are no longer resonant. The maximum effective tune corresponds to particles with amplitude equal to eight times the *rms* amplitude because there are not enough particles at greater amplitudes to affect the beam. Substituting Eq. (19) into Eq. (18), with the limits on maximum and minimum effective tuneshifts, and solving for the design tunes, we get

$$c - \delta\nu(8\varepsilon_n) + 0.125\Delta\nu_{\max} < a\nu_{xo} + b\nu_{yo} < c + \delta\nu(2\varepsilon_n) + 0.632\Delta\nu_{\max}, \tag{20}$$

where $\delta\nu(A) \equiv a\delta\nu_x + b\delta\nu_y$ at amplitude A, $\Delta\nu \equiv a\Delta\nu_{x,max} + b\Delta\nu_{y,max}$, and $\varepsilon_n$ is the normalized emittance.

Equation (20) is the region of instability for coupled resonance. The thickness of the unstable region is governed by the width of the unstable region ($\delta\nu$) as well as the width of the tune spread ($\Delta\nu_{max}$).

## CONCLUSIONS

In the presence of space charge, the integer resonance instability of particle orbits in a synchrotron occurs when large amplitude particles ($1<A<8$) have a rational value. When small amplitude particles are resonant the beam size remains constant while the particles redistribute from a Gaussian to a more linear distribution. The beam restabilizes when, due to the redistribution by the instability for some class of particles, no particles have resonant tunes.

The coupled resonance also has a finite region of instability. Without space charge the instability has an amplitude dependent, finite width. The instability exhibits both an exponential growth within the critical tunes of the resonant tune, as well as a sinusoidal growth outside the critical tune. The amplitude of the exponential and sinusoidal emittance growth at a given time is inversely proportional to the distance from the resonance tune.

When space charge is included the beam becomes unstable and the synchrotron loses particles when large amplitude particles lie within the region of exponential growth. When the large amplitude particles lie in the sinusoidal region the average emittance

increases due to the sinusoidal particle amplitudes, but the beam does not lose any particle.

This work is in part supported by the U.S. Department of Energy.

[1] T.P. Wangler. *Space Charge Dominated Beams and Applications of High Brightness Beams, Bloomington, IN, 1995* edited by S.Y. Lee, **AIP-377** (1996).

[2] S.Y. Lee. *Proceedings, International Workshop on Particle Dynamics in Accelerators: Emitance in Clrcular Accelerators, Tsukuba, Japan, 1994*, edited by S. Machida and K. Hirata. KEK, Tsukuba, Japan, 1 (1995).

[3] A. Chao. *Physics of Collective Beam Instabilities in High Energy Accelerators*. (John Wiley & Sons, New York, 1993).

[4] E.D. Courant and H.S. Snyder, *Ann. Phys.* **3**, 1 (1958).

[5] L.J. Laslett, *Proceedings, Summer Study on Storage Rings, Brookhaven National Laboratory, 1963.* **BNL-7534**, 324 (1963).

[6] R. Baartman, *Proceedings, International Workshop on Particle Dynamics in Accelerators: Emitance in Circular Accelerators, Tsukuba, Japan, 1994*, edited by S. Machida and K. Hirata. KEK, Tsukuba, Japan, 273 (1995).

[7] M.B. Ottinger. *Resonant Instabilities in Synchrotron Accelerators with Space Charge*. Doctoral Dissertation, University of Texas (1997).

[8] M.B. Ottinger and T.Tajima. *Space Charge Tracking Code for a Synchrotron Accelerator*. University of Texas IFSR#789 (1997).

[9] L. Schachinger and R. Talman, *Particle Accelerator* **22**, 35 (1987).

[10] S. Machida. *Proceedings, Computational Accelerator Physics Conference, Pleasanton, CA, 1993*, edited by R. Ryne, **AIP-297** (1993).

[11] C. Chen and R.A. Jameson, *Phys. Rev. D* **52**, 3074 (1995)

Figure 1: Comparison of Region of Instability for three beam configurations with the same space charge tuneshift. (Test 1: 10 MeV, 0.50 Amp, $10\pi$ mm-mrad; Test 2: 20 MeV, 1.00 Amp, $10\pi$ mm-mrad; Test 3: 10 MeV, 0.25 Amp, $5\pi$ mm-mrad)

Figure 2: Comparison of Region of Instability for Four Currents

Figure 3: Time Evolution of (a) Vertical Beam Emittance and (b) Average Vertical Tune for Several Design Tunes.

Figure 4: Scatter plots of initial [(a),(d),(g),& (j)] and final [(b),(e),(h), & (k)] tune distributions, and initial and final radial profiles [(c ), (f ), (i), & (l)] for design tunes [(a)-(c ) $\nu$=1.01, (d)-(f) $\nu$=1.05, (g)-(i) $\nu$=1.09, (j)-(l) $\nu$=1.15]

Figure 5: Regions of Instability (without space charge) as a function of Particle Amplitude and Design Tune

Figure 6: Amplitude as a function of turn for 8 different design tunes, without space charge.

Figure 7: Amplitude Evolution for Vertical Machine Tune of 1.12 [Initial Tune-Amplitude Distribution, Final Tune-Amplitude Distribution, Amplitudes for a sample of 250 particles as a function of turn]

Figure 8: Amplitude Evolution for Vertical Machine Tune of 1.14 [Initial Tune-Amplitude Distribution, Final Tune-Amplitude Distribution, Amplitudes for a sample of 250 particles as a function of turn]

Figure 9: Amplitude Evolution for Vertical Machine Tune of 1.15 [Initial Tune-Amplitude Distribution, Final Tune-Amplitude Distribution, Amplitudes for a sample of 250 particles as a function of turn]

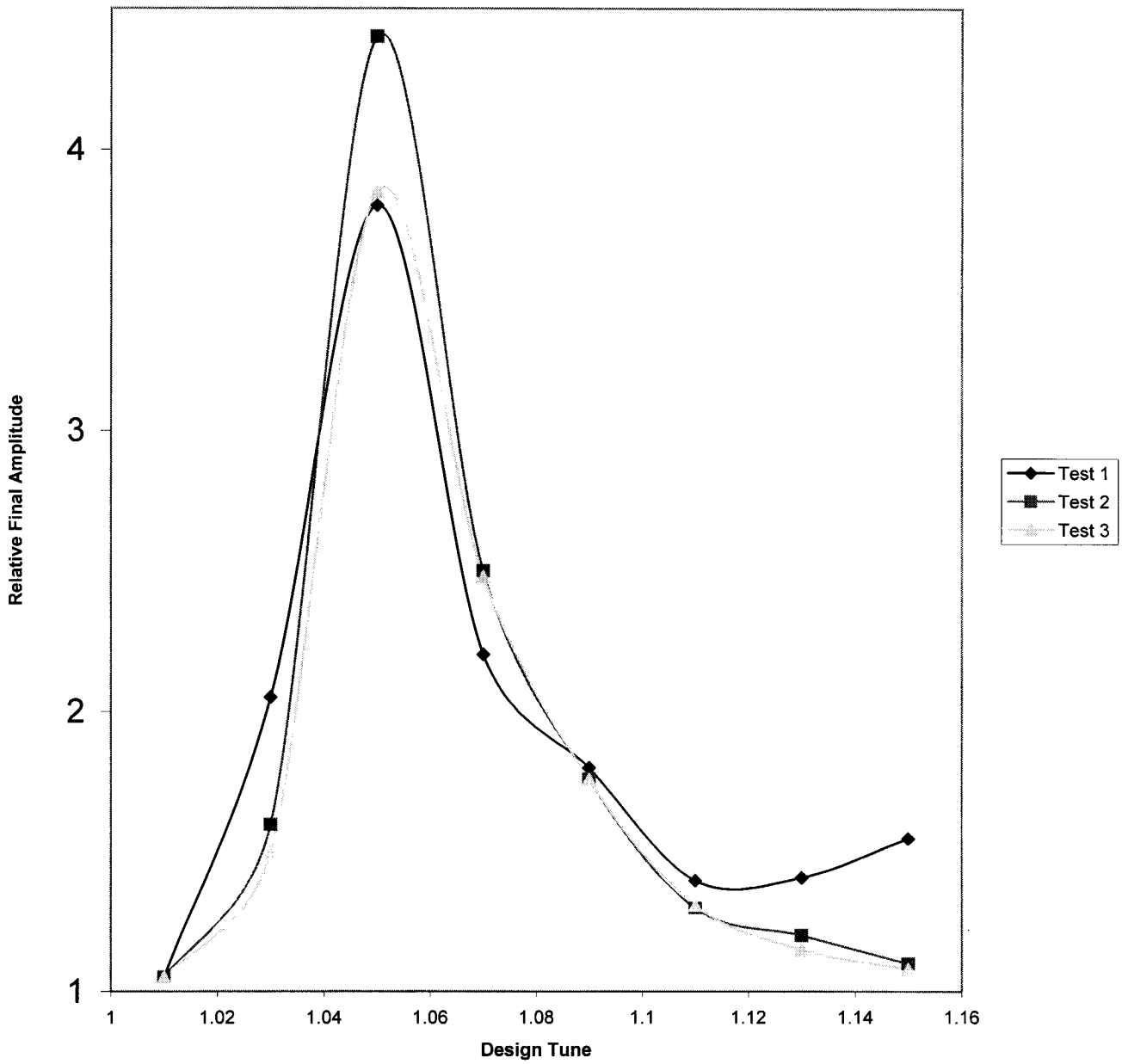


Michael B. Ottinger

Figure 1

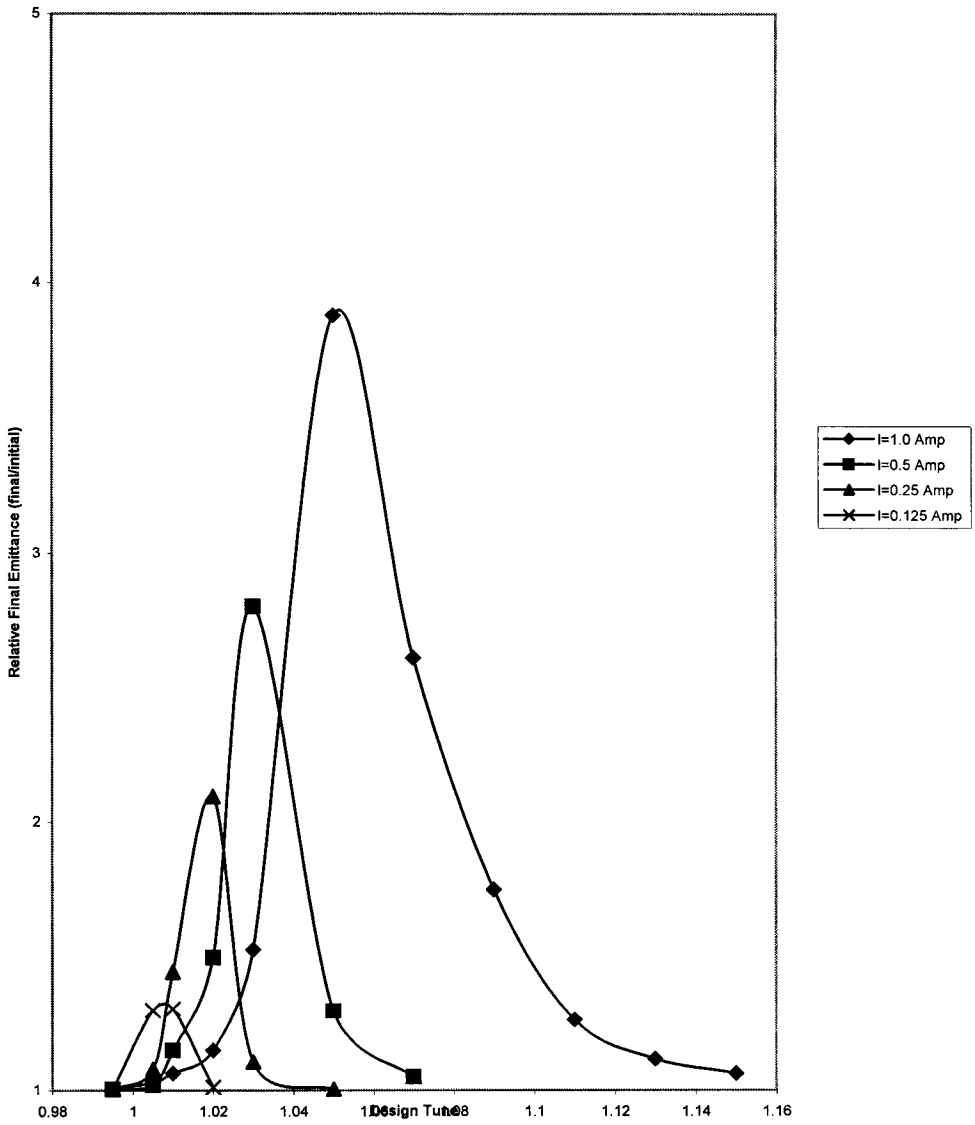
5
4
3
2
1
Relative Final Emittance (final/initial)
0.98
1
1.02
1.04
1.06
1.08
1.1
1.12
1.14
1.16
Design Tune
I=1.0 Amp
I=0.5 Amp
I=0.25 Amp
I=0.125 Amp

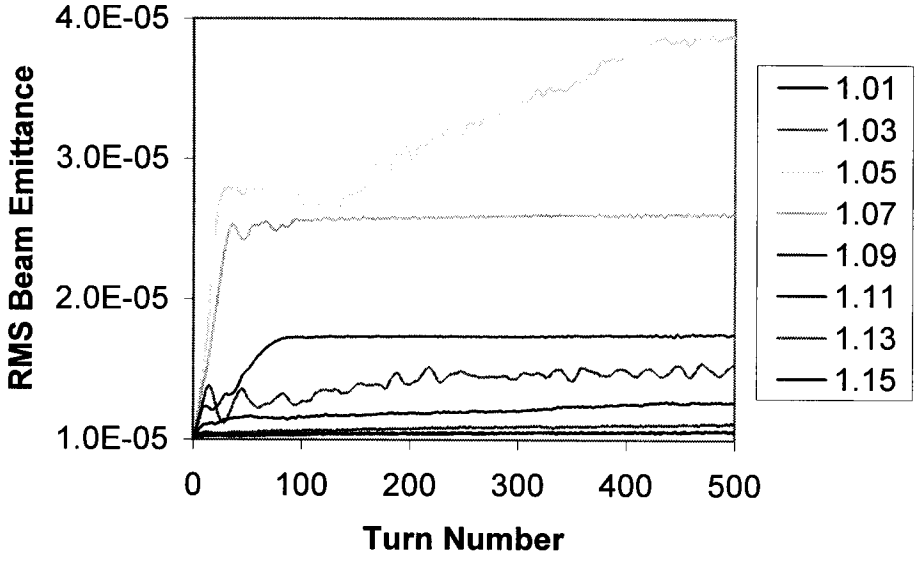


(a)

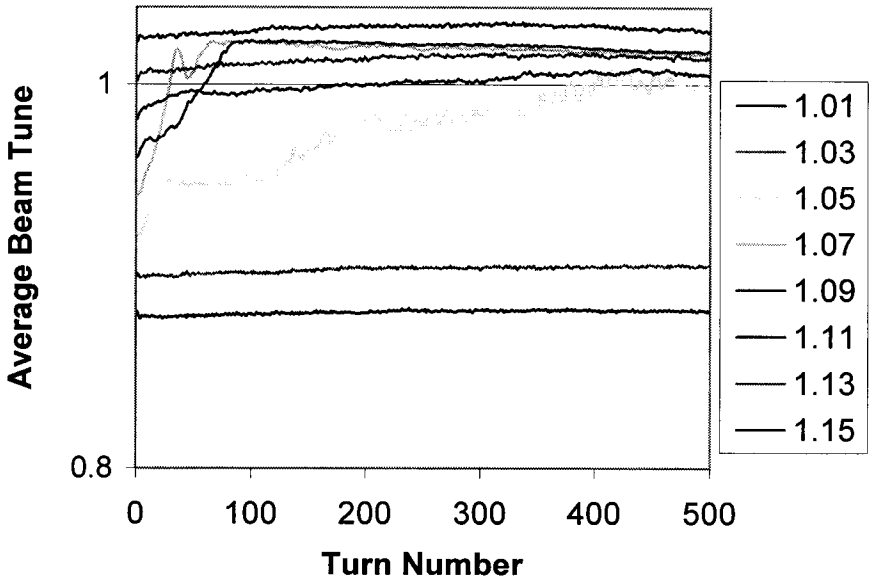


(b)

Michael B. Ottinger

Figure 3

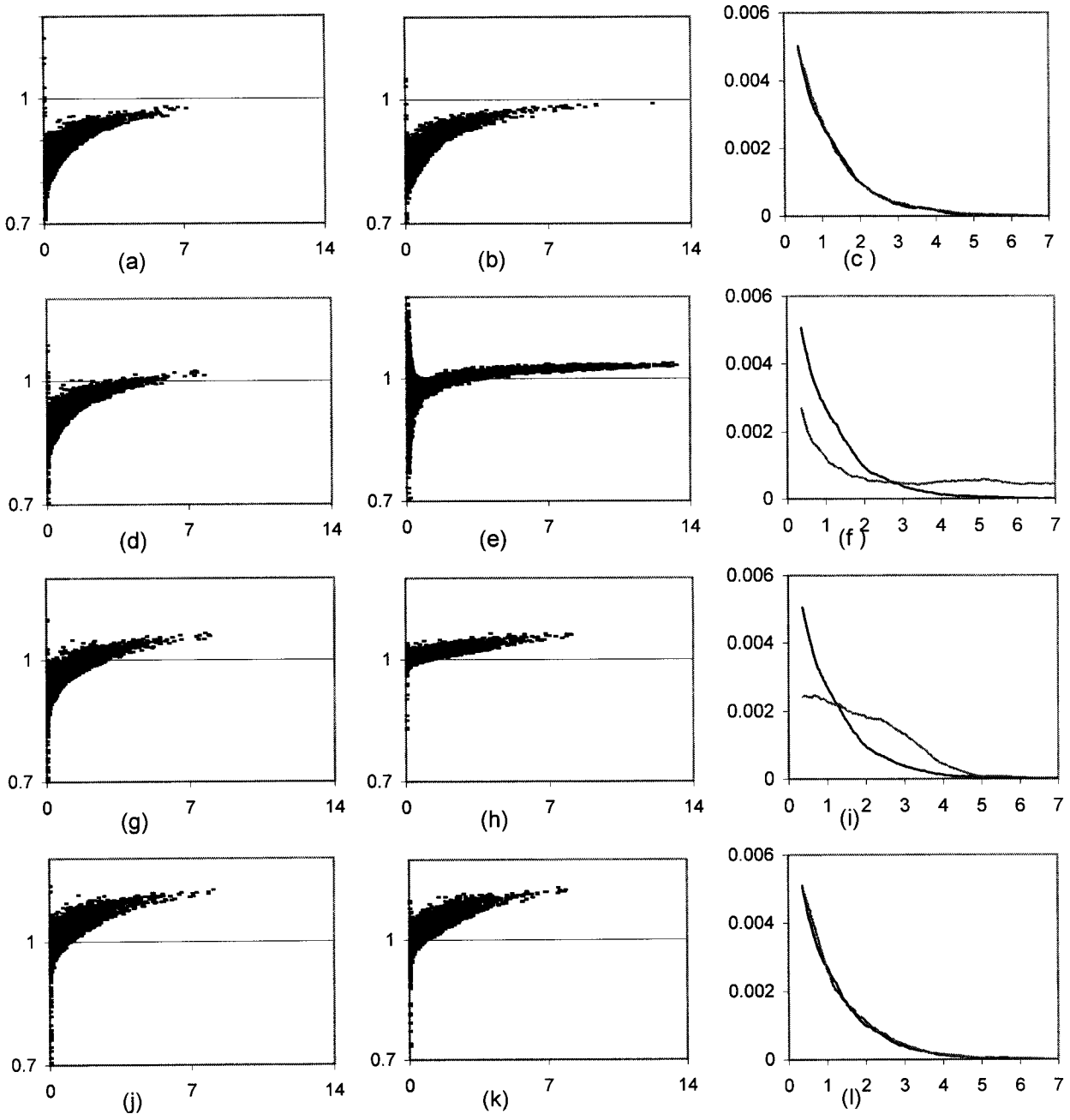


Michael B. Ottinger

Figure 4

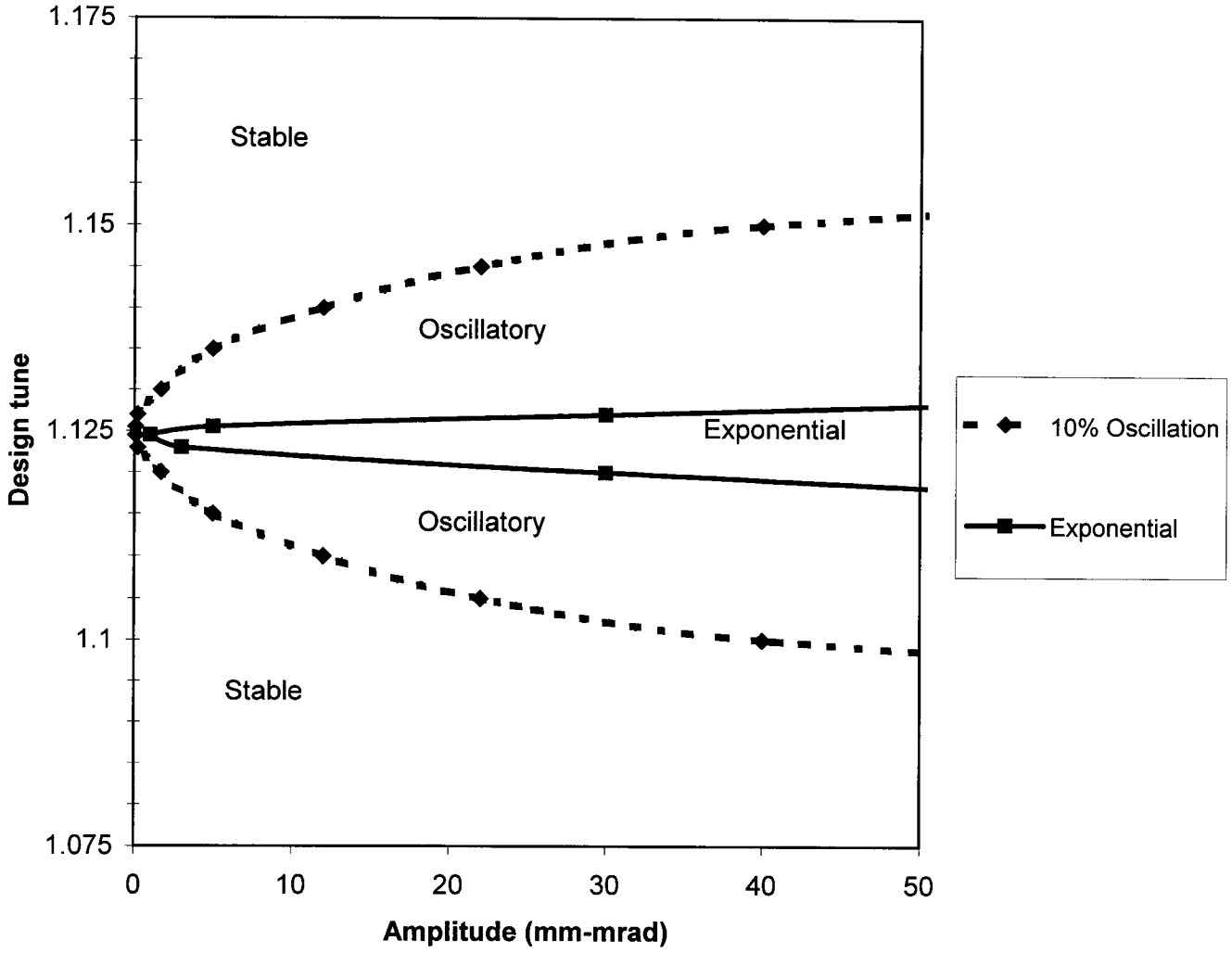


Michael B. Ottinger

Figure 5

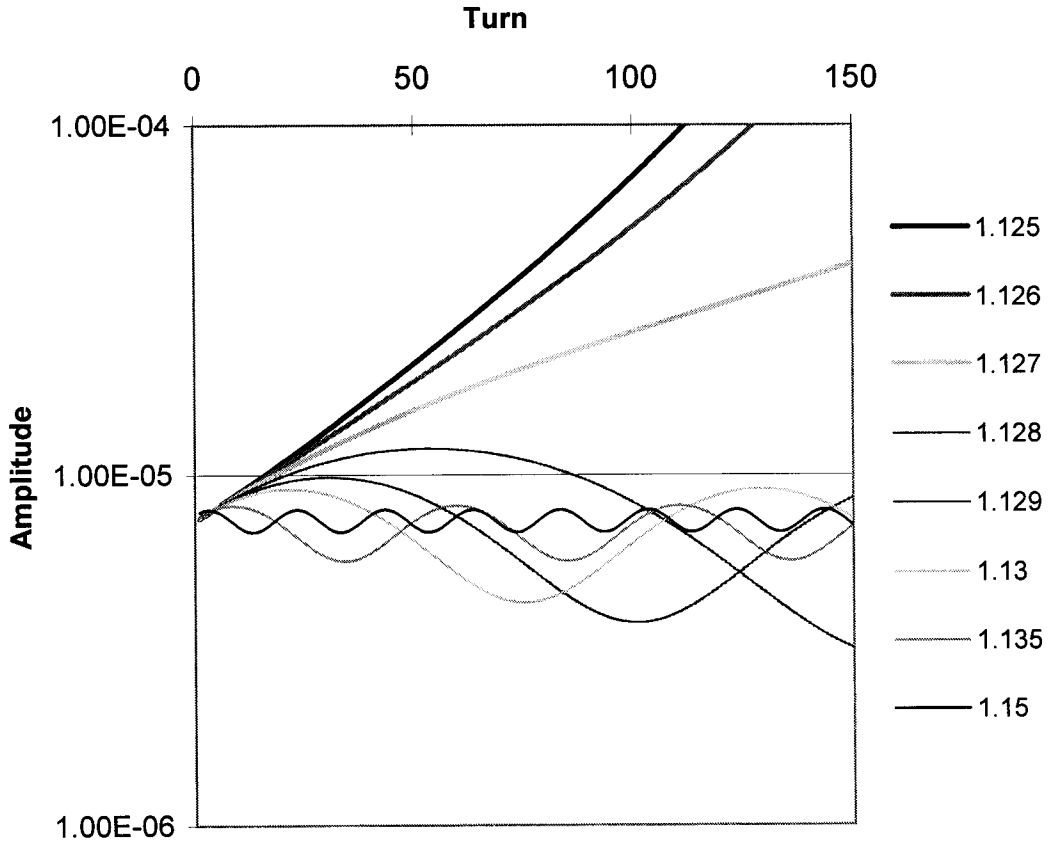


Michael B. Ottinger

Figure 6

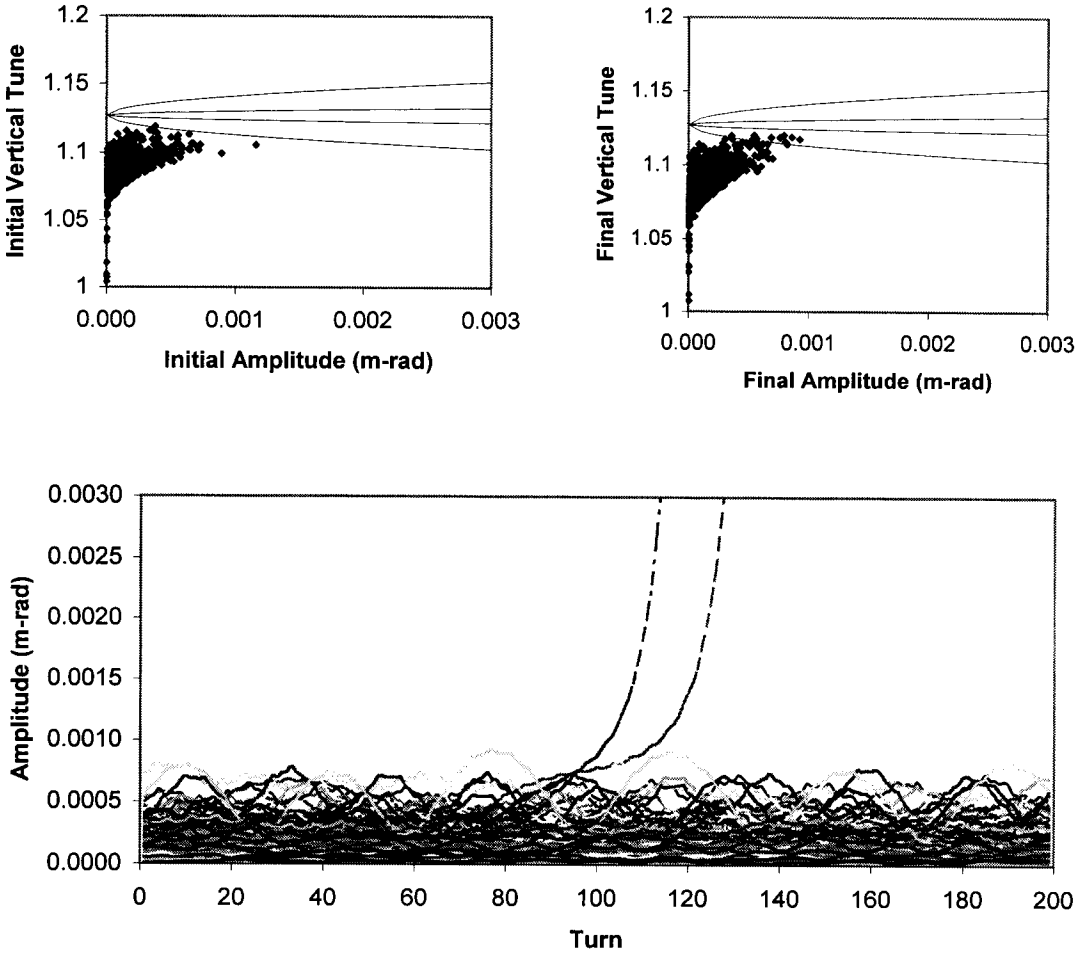


Michael B. Ottinger

Figure 7

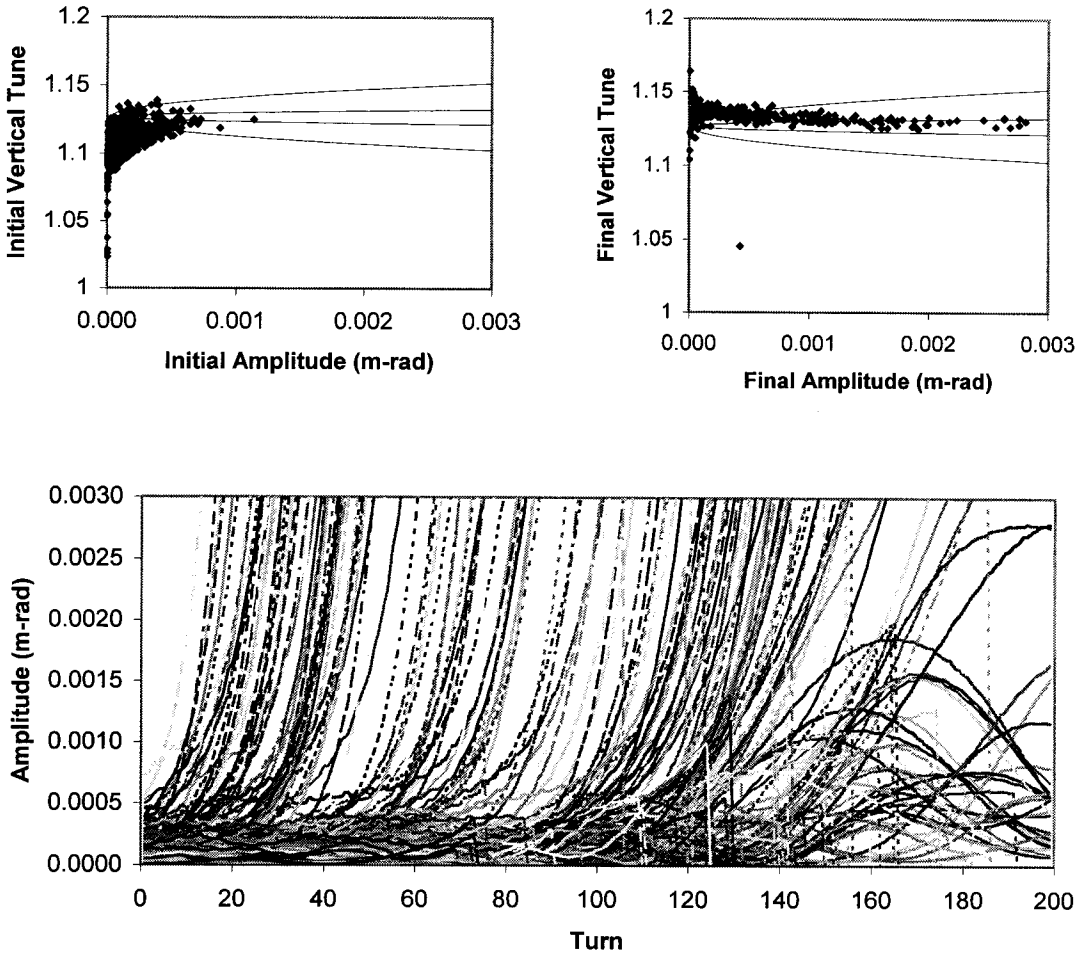


Michael B. Ottinger

Figure 8

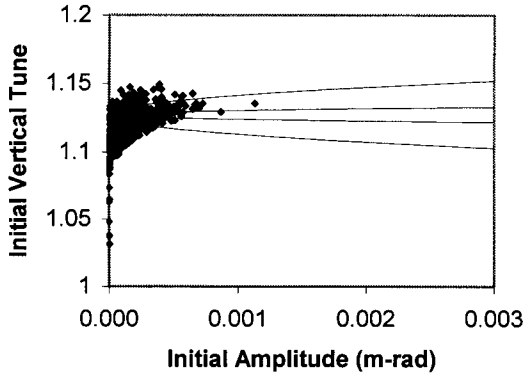


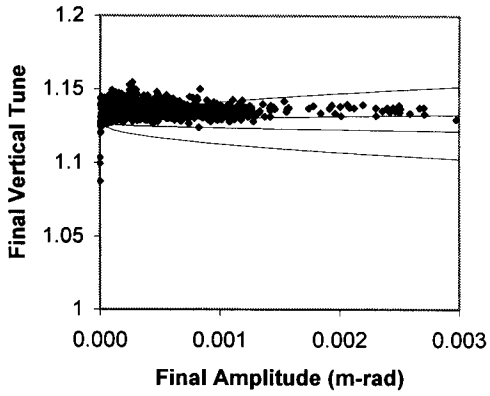


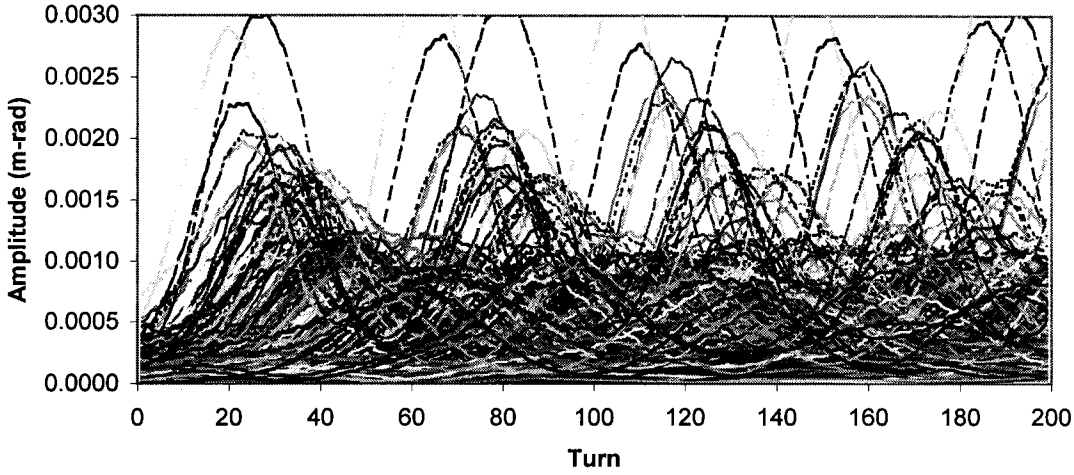


Michael B. Ottinger

Figure 9